

# Simulation of large parallel plasma flows in the tokamak SOL driven by cross-field transport asymmetries

A.Yu. Pigarov <sup>a,\*</sup>, S.I. Krasheninnikov <sup>a</sup>, B. LaBombard <sup>b</sup>, T.D. Rognlien <sup>c</sup>

<sup>a</sup> *University of California at San Diego, UCSD Center for Energy Research, EBU-II, 9500 Gilman Dr., La Jolla, CA 9209-0417, United States*

<sup>b</sup> *Massachusetts Institute of Technology, Cambridge, MA, United States*

<sup>c</sup> *Lawrence Livermore National Laboratory, Livermore, CA, United States*

---

## Abstract

Large-Mach-number parallel plasma flows in the single-null SOL of different tokamaks are simulated with multifluid transport code UEDGE. The key role of poloidal asymmetry of cross-field plasma transport as the driving mechanism for such flows is discussed. The impact of ballooning-like diffusive and convective transport and plasma flows on divertor detachment, material migration, impurity flows, and erosion/deposition profiles is studied. The results on well-balanced double null plasma modeling that are indicative of strong asymmetry of cross-field transport are presented.

© 2007 Elsevier B.V. All rights reserved.

*PACS:* 52.55.Fa; 52.40.Hf; 52.25.Vy; 52.30.Ex; 52.30.–q

*Keywords:* Cross-field transport; Plasma flow; Edge plasma; Impurity transport; UEDGE

---

## 1. Introduction

Recent experiments on several tokamaks and supporting theoretical studies have showed the strong cross-field plasma convection (due to intermittent edge turbulence) as well as the existence of large parallel plasma flows (LPPFs) in the SOL of single null (SN) and unbalanced double null (UDN) magnetic configurations. Detailed experimental characterization of SN and UDN discharges in Alcator C-Mod indicates [1] that LPPFs originate in the SOL near the low-field side (LFS) mid-plane and accelerate

to near sonic speed at the high field side (HFS) mid-plane toward the HFS divertor. These C-Mod observations and some related experiments on other tokamaks have revealed an important edge-physics phenomenon: the dominant driving mechanism of LPPFs appears to be a strong ballooning-like asymmetry in the anomalous cross-field (ACF) plasma transport. Moreover, substantially different radial profiles of plasma parameters measured at the LFS and HFS mid-planes in the well-balanced DN discharges on C-Mod can also be explained by the strong LFS/HFS asymmetry in ACF transport. Recent theoretical analysis by Pigarov et al. [2,3] using the UEDGE code has confirmed the importance of ACF asymmetry in generating the LPPFs.

---

\* Corresponding author.

*E-mail address:* [apigarov@ucsd.edu](mailto:apigarov@ucsd.edu) (A.Yu. Pigarov).

In the paper, we present results of multi-fluid modeling with UEDGE code of large parallel plasma flows in the SOL that demonstrate the outstanding role of ballooning-like asymmetry in cross-field plasma transport as the driving mechanisms of such flows. The impact of LPPFs on divertor detachment, material migration, impurity flows, and erosion/deposition profiles is studied.

## 2. Anomalous cross-field transport model in UEDGE

The UEDGE code is used for extensive simulations of edge plasma and neutral gas transport (including multi-species, multi-ion, fluid equations along magnetic field lines, realistic non-orthogonal 2D mesh based on tokamak equilibrium). We employ diffusive-and-convective model [2] for ACF plasma transport. Intermittent (e.g., due to blobs and holes) transport effect is modeled by means of anomalous convective velocity  $V_{\text{conv}}$ . Ion charge states may have different sign and amplitude of  $V_{\text{conv}}$  [2]. The model introduces asymmetric (e.g., ballooning-like) 2D profiles for all transport coefficients, which are adjusted to match a representative set of experimental data. Being a smooth function along the magnetic flux surface (MFS), the profile of  $V_{\text{conv}}$  is characterized by asymmetry factor  $\eta_{\text{as}}(V) = V_{\text{conv}}(\text{IMP})/V_{\text{conv}}(\text{OMP})$ , where IMP and OMP stand for the inner and outer mid-planes. Profiles of plasma diffusivities,  $D_{\perp}$  and  $\chi_{\perp}$ , may have

their own asymmetry factors,  $\eta_{\text{as}}(D)$  and  $\eta_{\text{as}}(\chi)$ . No classical drifts are used here and a discussion on the effect of drifts on LPPFs will be presented in elsewhere.

## 3. Cross-field transport asymmetry as the LPPF driving mechanism

In our model, the cross-field transport, which is mainly due to plasma convection by blobs in the SOL, is strongly peaked around the LFS mid-plane with magnitude of  $V_{\text{conv}}$  increasing in the radial direction. Near the wall, the peak  $V_{\text{conv}}$  typically is a few hundred  $m/s$  at OMP and is few tenths  $m/s$  at IMP. The fast and spatially localized transport pushes plasma into the far SOL, so that, the total (gas + plasma) pressure profile along magnetic field lines may have pronounced maximum (1.5–2X) at the OMP, thus, causing the parallel plasma flows into the inner and outer divertors. This flow-driving mechanism is demonstrated in Fig. 1 by displaying some results of UEDGE modeling of the C-Mod discharge having been considered in [3]. Inspecting profiles of plasma parameters, total pressure, velocity  $V_{\parallel}$ , Mach number  $M_{\parallel}$ , and flux  $\Phi_{\parallel}$  of plasma in parallel direction and comparing the profiles in the far SOL to the profiles in the middle of SOL, one sees that (i) plasma flow at the magnetic surface closer to separatrix results in the plasma pressure equilibration due to high recycling on the divertor plates followed by the flow stagnation (notice, the

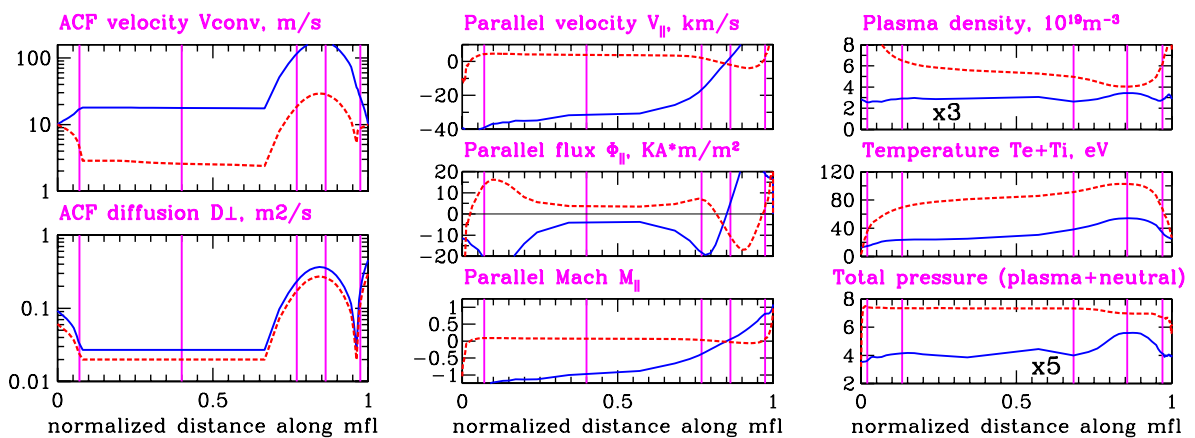


Fig. 1. Plasma parameter profiles along magnetic field lines (MFLs) in the SOL (0 and 1 abscissa values correspond to the inner and outer divertor plates) calculated with UEDGE,  $\eta_{\text{as}} = 0.1$ , for a SN shot in C-Mod are shown on middle and right panels. Left panels display the input profiles of  $V_{\text{conv}}$  and  $D_{\perp}$ . Broken (red online) curves show the profiles for a MFL in the middle of SOL ( $\rho = 0.5$  cm), whereas solid curves represent profiles in the far SOL ( $\rho = 1.3$  cm). Five vertical lines correspond to locations of (from left to right) entrance to inner divertor, IMP, plasma top, OMP, and entrance to outer divertor. Negative values of  $V_{\parallel}$ ,  $M_{\parallel}$ ,  $\Phi_{\parallel}$  correspond to the flow toward the inner plate. (For interpretation of the figure in color, the reader is referred to the web version of this article.)

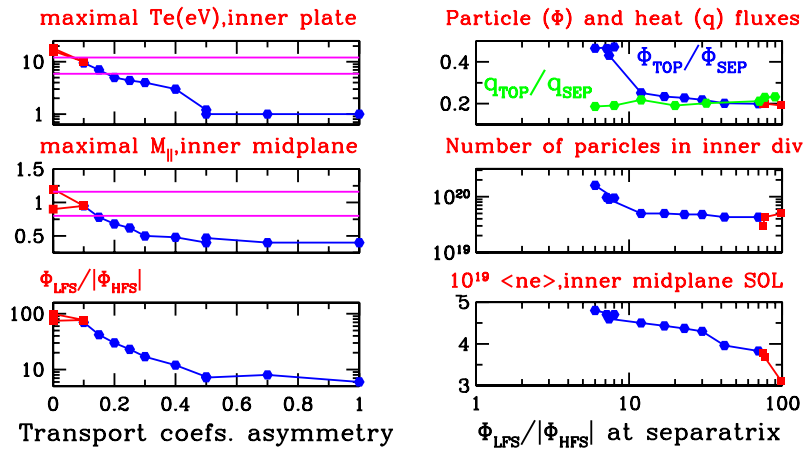


Fig. 2. The maximal  $T_e$  at the inner plate,  $M_{\parallel}$ , and the ratio  $\Phi_{LFS}/|\Phi_{HFS}|$  are displayed versus asymmetry factor  $\eta_{as}$  of cross-field transport on the left panels. The UEDGE calculations were done for typical C-Mod SN L-mode shot. Experimental data are scattered within two horizontal lines. In the right panels, the calculated ratios ( $\Phi_{TOP}/\Phi_{SEP}$  and  $q_{TOP}/q_{SEP}$ , where  $\Phi_{TOP}$ ,  $q_{TOP}$  and  $\Phi_{SEP}$ ,  $q_{SEP}$  are the total particle and energy fluxes carried by the LPPF and transported through separatrix), number of particles in the inner divertor, and averaged SOL plasma density are shown versus  $\Phi_{LFS}/|\Phi_{HFS}|$ , the real LFS/HFS flux asymmetry.

OMP pressure maximum is small, since  $n_e$  decrease is compensated by increase in  $T_e + T_i$ , whereas (ii) plasma flow at the magnetic surface in the far SOL accelerates to about sonic speed by parallel pressure gradient due to relatively weak plasma collisionality, low-viscosity, and easier leakage of neutral (or plasma) particles back to core from inner divertor (notice, at the OMP both  $n_e$  and  $T_e$  are peaked maintaining the pressure maximum which is 1.5X the background pressure at this MFS).

As boundary conditions at the outermost flux surface ('wall') in UEDGE, we prescribe the values of cross-field scale length  $L_{\perp}$  of plasma parameters ( $n_i$ ,  $T_e$ ,  $T_i$ , and  $V_{\parallel}$ ). Typically  $L_{\perp}$  is several cm for  $n_e$  and  $T_e$ , and we use the same scale for  $V_{\parallel}$ . In most UEDGE runs, variation of  $L_{\perp}$  for  $V_{\parallel}$  from centimeters to meters does not affect substantially  $\Phi_{\parallel}$ .

As simulated with UEDGE, the LFS-to-HFS plasma flow exists in the SN in a wide range of  $\eta_{as} < 0.8$ . However, only low-values  $\eta_{as} \approx 0.1$  (leading to large LFS/HFS flux asymmetry  $\Phi_{LFS}/|\Phi_{HFS}| > 70$ ) are consistent with experimental data as shown in Fig. 2(left) for this C-Mod discharge. Note, that we use the modulus of particle flux coupled to the HFS area of separatrix, since at low  $\eta_{as}$  the net particle flux  $\Phi_{HFS} < 0$  is into the core due to plasma backflow from the inner divertor near the separatrix. The variation of LPPFs characteristics with  $\eta_{as}$  is shown in Fig. 2(right). As seen, the LPPF carries  $\approx 20\%$  of plasma particles and energy entering the SOL through the separatrix. At large flux

asymmetries  $\Phi_{LFS}/|\Phi_{HFS}|$  (i.e., low  $\eta_{as}$ ) the particle flux is relatively small, so that for the given power input, the inner divertor is attached as it is in this discharge. In this case, flow velocity is the highest and maximal  $M_{\parallel}$  can reach unity. With increasing in  $\eta_{as}$ , primarily results in a strong increase of particle flux into the inner divertor, the IMP radial profile of plasma density broadens and the plasma collisionality and divertor opacity to neutrals increase in the entire SOL, so that, the plasma flow tends to stagnate also in the far SOL region. In the case when ACF transport is more or less poloidally symmetric, the inner divertor leg is detached.

#### 4. Role of LPPF in impurity migration and deposition

Impurity sources and parallel flows of impurity ions for LPPF conditions are simulated with UEDGE under the assumption of high LFS/HFS cross-field transport asymmetry. The impurity cross-field transport model assigns different anomalous convective velocities to charge states of plasma ions (parameter  $\eta_{CCC} = -1$  [2]) in order to match various experimental data. For L-mode discharges on NSTX, C-Mod and DIII-D tokamaks, our simulations have showed that high charge states ( $Z > 2$ ) of impurity ions are highly entrained in the far SOL by the background deuterium plasma flows from near the outer mid-plane into the divertors, as shown in Fig. 3(bottom). Velocities of the lowest charge states,

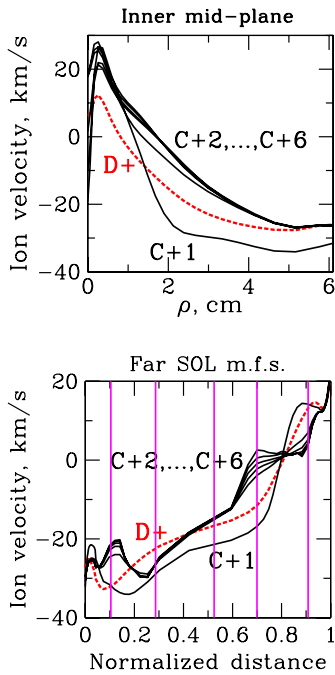


Fig. 3. Top panel displays radial profiles of ion flow velocities for background plasma (red, broken) and for different impurity ion charge states (solid curves). These profiles are related to SOL at the IMP, whereas the coordinate  $\rho$  is mapping the magnetic flux surfaces to their distance from separatrix at the OMP. Bottom panel displays the variations of ion velocities with distance along the magnetic field line from inner to outer divertor plates in the far SOL ( $\rho = 0.8$  cm). The UEDGE calculations were done for low-density SN L-mode shot in DIII-D,  $\eta_{as} = 0.1$ ,  $\eta_{CCC} = -1$ . (For interpretation of the figure in color, the reader is referred to the web version of this article.)

$C^{1+}$  and  $C^{2+}$ , have the largest deviation ( $\sim 2X$ ) from plasma velocity, since they are also affected by both

impurity sources and strong cross-field convective transport directed inwardly. In the far-SOL region at IMP where LPPFs are strong, Fig. 3(top) shows that the impurity ions tend to have the same profile of flow velocity as the deuterium ions. Note, in the far SOL, impurities are highly supersonic when the deuterium plasma flow is near-sonic.

For the typical LSN shot on C-Mod with measured LPPF, the diagram of impurity fluxes inferred from UEDGE simulations is shown in Fig. 4(middle). As seen, the outer chamber wall exhibits large net erosion ( $21.4 - 5.12 = 16.3$  A). This strong erosion is due to sputtering by intermittent convective cross-field plasma flux. In material migration analysis, the outer wall is the dominant donor of impurities, whereas the outer and inner divertor plates are the net sinks for impurities. The net particle deposition on the outer and inner plates are 11 A and 5 A, respectively, and their sum, 16 A, is roughly equal to the wall net erosion. Large parallel plasma flow carries 5 A onto the inner divertor plate, that is,  $\sim 20\%$  of all impurity ions sputtered from the outer wall. The material sputtered from outer wall (11 A) consists of 25% of the outer plate erosion rate (42 A). Impurities from the outer wall are shared between inner and outer divertors roughly in the same ratio as the cross-field plasma flux does when passing through separatrix.

The UEDGE modeling of this shot also shows that impurities sputtered from outer chamber wall are transported by LPPF into the inner divertor mainly in the far SOL region. The calculated profiles of impurity erosion and deposition at the inner plate are shown in Fig. 4(right). As seen, in the far SOL,  $\rho > 0.5$ , the erosion rate decreases with  $\rho$  since

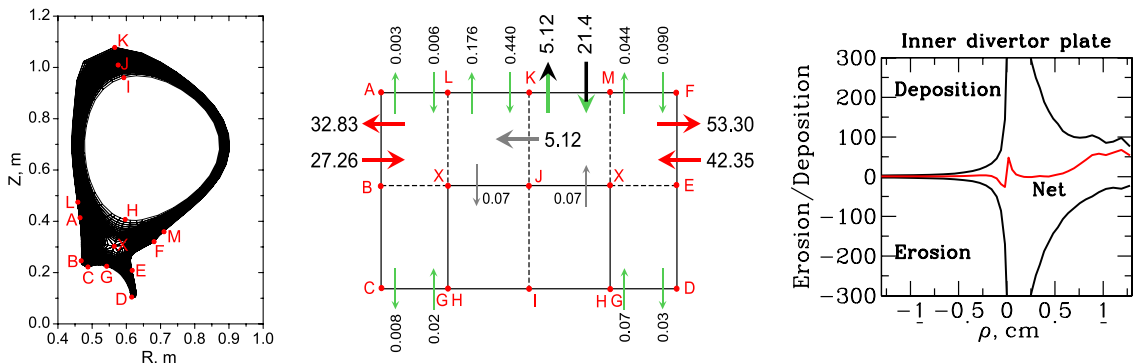


Fig. 4. The impurity flow diagram calculated with UEDGE (middle panel) for C-Mod SN discharge,  $\eta_{as} = 0.1$ ,  $\eta_{CCC} = -1$ . The letters stand for characteristic points in the computational mesh which is shown on left panel. Radial profiles of erosion (negative curve), deposition (positive), and net deposition rates at the inner divertor plate are displayed on the right panel as functions of  $\rho$ , the distance from separatrix to magnetic flux surface at the OMP,  $\rho > 0$  correspond to the SOL.

the plasma temperature and flux decrease there, whereas the deposition rate is relatively constant. Erosion/deposition rates are largely peaked near the strike points, whereas the net deposition is small compared to the deposition in the far SOL. As modeled, the largest *net deposition rates* are attained in the far SOL region due to impurities carried by LPPFs on the divertor plates. The net deposition profile predicted by UEDGE to be peaked in the far SOL region is in agreement with some tokamak experiments, for example, Be deposition on C in the inner divertor in JET [4] and W on C in ASDEX.

### 5. Cross-field transport asymmetry in DN configuration

Experiments with an unbalanced double-null (DN) magnetic configuration on C-Mod show (as measured by reciprocating probes at the LFS and HFS mid-planes) that plasma density profiles have a much shorter cross-field decay length in the region outside the secondary separatrix on the HFS compared to the same region on the LFS [5]. In well-balanced DN discharges, the density e-folding length measured at the HFS mid-plane is substantially smaller than that in the SN configuration (Fig. 5). These data independently indicate a strong ballooning-like asymmetry where the cross-field plasma flux is much larger on the LFS.

The UEDGE modeling of well-balanced DN C-Mod shots is used to infer an asymmetry factors for the anomalous cross-field plasma (diffusive and convective) transport from matching experimental

profile data. Firstly, for fixed  $D_{\perp}$  and  $\chi_{\perp}$ , we vary the asymmetry of convective velocity in two ways: (i) scan values of  $V_{\text{conv}}(\text{IMP})$  at IMP while  $V_{\text{conv}}(\text{OMP})$  at OMP is fixed, and (ii) vary  $V_{\text{conv}}(\text{OMP})$  and asymmetry factors  $\eta_{\text{as}}(V)$  and select runs with the same total plasma flux through the separatrix where the flux is approximately given by ionization source from  $D_x$  measurements and by pressure measurements at the OMP. In both cases we find that small asymmetries, i.e.,  $\eta_{\text{as}} > 0.2$ , substantially overestimate the plasma density in the far SOL at HFS as well as the  $J_{\text{sat}}$  at inner plate. This result is exactly what one should expect from the very nature of blobby transport since in DN the LFS and HFS parts of SOL are completely disconnected. Secondly, we vary the peak value and asymmetry in profiles of all transport coefficients and obtain the best fit of UEDGE to experimental data. The best-fit results are shown in Fig. 5 for the LFS, HFS, and divertor probes data. In this case, convective transport at the HFS is small,  $\eta_{\text{as}} = 0.1$  (or even no blobby transport), and the asymmetry in plasma diffusivities is also large,  $\eta_{\text{as}}(D, \chi) = 0.2$ . Notice that experimental profiles are reproduced by UEDGE reasonably well in a wide range  $0.1 < \eta_{\text{as}}(D, \chi) < 0.4$ , and the accuracy of experimental data does not allow a better resolution of transport asymmetry. The smaller asymmetry factors  $\eta_{\text{as}}(D, \chi) < 0.1$  result in the inner leg detachment since small power is transported into the HFS SOL, whereas the values larger than 0.4 cause significant overestimation of  $J_{\text{sat}}$ .

Finally, our previous study [3] of SN discharges on C-Mod found that the ballooning-like

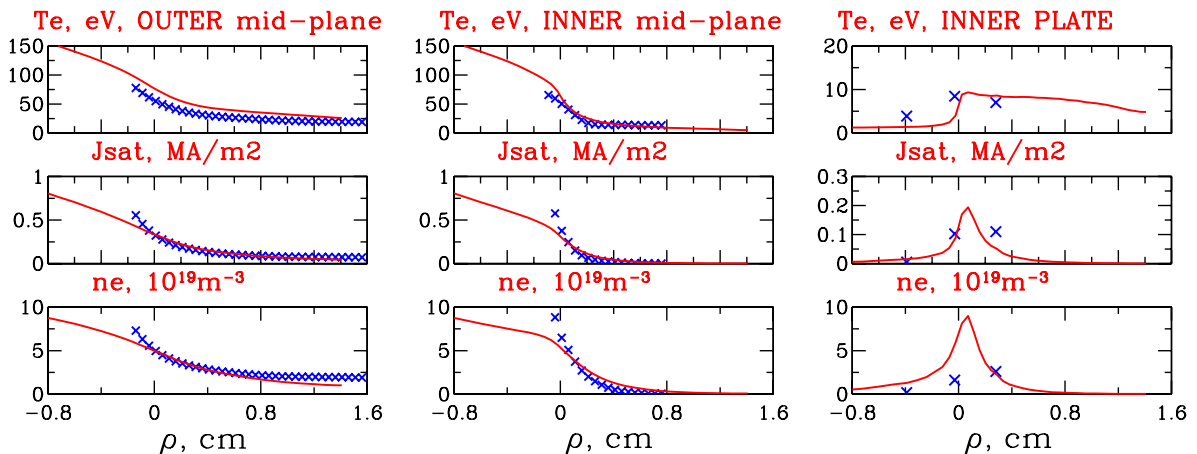


Fig. 5. The results of UEDGE simulations (solid curves) are compared with experimental profiles (crosses) of plasma density  $n_e$ , ion saturation current  $J_{\text{sat}}$ , and temperature  $T_e$  at LFS mid-plane (left), HFS mid-plane (middle) and HFS divertor plate (right panel) as measured by reciprocating and Langmuir probes in C-Mod for well-balanced DN.

asymmetries were necessary assigned in SN to both  $V_{\text{conv}}$  and diffusivities. The asymmetry factors deduced from matching all five probe systems on C-Mod in those shots with UEDGE were in the range  $\eta_{\text{as}}(V_{\text{conv}}) \approx \eta_{\text{as}}(D, \chi) = 0.1\text{--}0.15$  which is consistent with our results for the present DN case.

## 6. Conclusions

The edge plasma transport modeling with UEDGE shows that ballooning-like cross-field blobby transport results in large-Mach-number parallel plasma flows in the far SOL. The HFS/LFS

asymmetry of ACF transport coefficients deduced from simulations of experimental data in both SN and well-balanced DN is large,  $\eta_{\text{as}} = 0.1\text{--}0.2$ . The parallel flows have large impact on impurity migration and on detachment of inner divertor.

## References

- [1] B. LaBombard et al., Nucl. Fusion 44 (2004) 1047.
- [2] A.Yu. Pigarov et al., J. Nucl. Mater. 337–339 (2005) 371.
- [3] A.Yu. Pigarov et al., Contrib. Plasma Phys. 46 (2006) 229.
- [4] M. Rubel et al., J. Nucl. Mater. 313–316 (2003) 321.
- [5] C.J. Boswell et al., Plasma Phys. Control. Fusion 46 (2004) 1247.